Fibre Optic Nonlinear Technologies [FONTE]

- A European Industrial Doctorate [GA766115]

Document Details

Title	Deliverable 5.4 NFT-WDM transmission systems
Deliverable number	D5.4
Deliverable Type	Report (public)
Deliverable title	NFT-WDM transmission systems
Work Package	WP5 – Experimental implementation and testing of NFT system
Description	
Deliverable due date	30/04/2021
Actual date of submission	25/03/2022
Lead beneficiary	TPT and ALUD (NBL)
Version number	V1.0
Status	FINAL

Dissemination level

PU	Public	X
CO	Confidential, only for members of the consortium (including Commission Services	

Project Details

Grant Agreement	766115
Project Acronym	FONTE
Project Title	Fibre Optic Nonlinear Technologies
Call Identifier	H2020-MSCA-ITN-2017
Project Website	fonte.astonphotonics.uk
Start of the Project	1 June 2018
Project Duration	48 months

Consortium

EC Funding

This project has received funding from the European Union's Horizon 2020 research and innovation programme under the Marie Skłodowska-Curie grant agreement No 76611

TABLE OF CONTENTS

LIST OF FIGURES

List of Acronyms

ADM Add drop multiplexer

AIR Achievable information rate

DBP Digital back-propagation

DoF degree-of-freedom

ISI Inter-symbol interference

INFT Inverse nonlinear Fourier transform

NFT Nonlinear Fourier transform

NFDM Nonlinear frequency division multiplexing

NLS Nonlinear Schrödinger

OFDM Orthogonal frequency division multiplexing

RX Receiver

TX Transmitter

WDM Wavelength division multiplexing

1 Executive Summary

We review linear and nonlinear frequency division multiplexing in optical fiber networks. We compare the achievable information rates (AIRs) of the wavelength-division multiplexing (WDM) and nonlinear frequency-division multiplexing (NFDM) in a network scenario. It is shown that the NFDM AIR is greater than the WDM AIR in a representative system with five users. The results presented in this report have been published in [2].

2 Introduction

One factor limiting data rates in optical communication is that linear multiplexing is applied to the nonlinear optical fiber. To address this limitation, NFDM was introduced [1, 3, 4]. NFDM is a signal multiplexing scheme based on the nonlinear Fourier transform (NFT), which represents a signal in terms of its discrete and continuous nonlinear Fourier spectra. In this approach, users' signals are multiplexed in the nonlinear Fourier domain and propagate independently in a model of the optical fiber described by the lossless noiseless nonlinear Schrödinger (NLS) equation.

To demonstrate NFDM high data rates, we consider the NLS equation in the defocusing regime, which has several advantages. First, the operator L in the Lax pair underlying the channel in the NFT is self-adjoint. Consequently, solitons, the less tractable part of the NFT, are absent. Second, numerical algorithms are robust in this regime. Third, the analyticity of the one of the nonlinear Fourier coefficients can be exploited to efficiently compute these coefficients from the NFT of signal. For this case, we show that the AIR of NFDM is greater than that of WDM, subject to a bandwidth and average signal power constraint.

3 Channel Model

The propagation of a signal in the single-mode single-polarization optical fiber with ideal distributed amplification can be modeled by the stochastic NLS equation. The equation in the normalized form reads [3, Eqs. 1–3]

$$j\frac{\partial q}{\partial z} = \frac{\partial^2 q}{\partial t^2} - 2s|q|^2 q + n(t, z), \tag{1}$$

where $q(t, z) : \mathbb{R} \times \mathbb{R}_0^+ \mapsto \mathbb{C}$ is the complex envelope of the signal as a function of time t and distance z along the fiber, $n(t, z)$ is (zero-mean) white circular symmetric complex Gaussian noise, and $j \triangleq \sqrt{-1}$. Here, $s \triangleq -1$ in the focusing regime (corresponding to the fiber with anomalous dispersion) and $s \triangleq +1$ in the defocusing regime (corresponding to the fiber with normal dispersion). The fiber length is denoted by $\mathcal{L}$.

In this review, we consider a *network environment*. This refers to a communication network with the following set of assumptions [1, Sec. II. B. 3]: (1) there are multiple transmitter (TX) and receiver (RX) pairs; (2) there are add-drop multiplexers (ADMs) in the network. The signal of the user-of-interest can co-propagate with the signals of the other users in part of the link. The location and the number of ADMs are unknown; (3) each TX and RX pair does not know the incoming and outgoing signals in the path that connects them. A link in a network environment is shown in Fig. 1.

To make use of the available fiber bandwidth, data in modulated in disjoint frequency bands in WDM. The AIRs of WDM — sometimes referred to as the "nonlinear Shannon limit — are presented in [5], [6] and references therein. Fig. 2 (a) shows the WDM AIR as a function of the average input power in a network environment. It can be seen that the AIR vanishes (or saturates in a modified scheme [7]) as the input power tends to infinity.

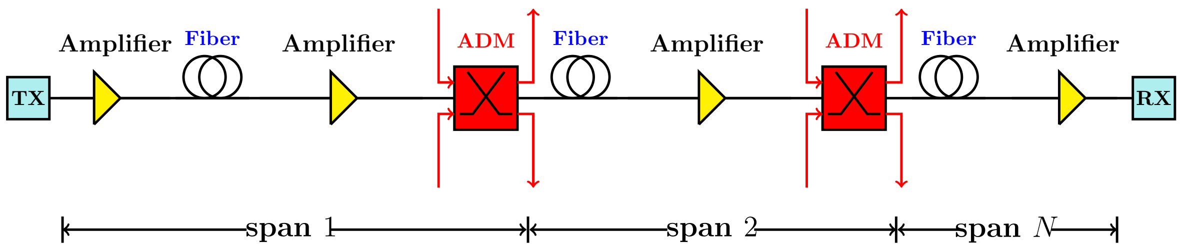

Fig. 1. An optical fiber link in a network environment.

In contrast to WDM, NFDM is fundamentally compatible with the channel [1,3,4]. NFDM exploits a particular structure in the channel model, in order to achieve interference-free communication. It is based on the observation that the deterministic NLS equation supports nonlinear Fourier "modes" which have an important property that they propagate independently in the channel, the key to build a multi-user system. The tool necessary to reveal independent signal degrees-of-freedom (DoFs) is the NFT. Based on the NFT, NFDM is constructed which can be viewed as a generalization of Orthogonal frequency division multiplexing (OFDM) in linear channels to the nonlinear optical fiber. Exploiting the integrability property, NFDM modulates non-interacting signal DoFs in the channel.

4 Nonlinear Frequency Division Multiplexing

In this section, we review NFT and NFDM from [2].

4.1 Review of the Nonlinear Fourier Transform

Let $T : \mathcal{H} \mapsto \mathcal{H}$ be a compact (linear) map on a separable complex Hilbert space $\mathcal{H}$ with the inner product $\langle ., . \rangle$. Consider the channel

$$Y \triangleq T(X) + N, \tag{2}$$

where X is the input signal, Y is the output signal and N is Gaussian noise on $\mathcal{H}$. The channel can be discretized by projecting signals and noise onto an orthonormal basis $(\phi_\lambda)_{\lambda \in \mathbb{N}}$ of $\mathcal{H}$

$$\{X, Y, N\} = \sum_{\lambda=1}^{\infty} \{X_\lambda, Y_\lambda, N_\lambda\} \phi_\lambda, \tag{3}$$

where $X_\lambda, Y_\lambda, N_\lambda \in \mathbb{C}$ are DoFs. This results in a discrete model

$$Y_\lambda = H_\lambda X_\lambda + \underbrace{\sum_{\mu \neq \lambda} H_{\lambda\mu} X_\mu}_{\text{linear interactions}} + N_\lambda, \tag{4}$$

where $H_{\lambda\mu} = \langle T\phi_\mu, \phi_\lambda \rangle$ and $H_\lambda \triangleq H_{\lambda\lambda}$. Depending on the choice of basis, interactions in (4) could refer to inter-symbol interference (ISI) in time, inter-channel interference in frequency, etc.

Suppose that T is diagonalizable and has a set of eigenvectors forming an orthonormal basis of $\mathcal{H}$, *e.g.* , when

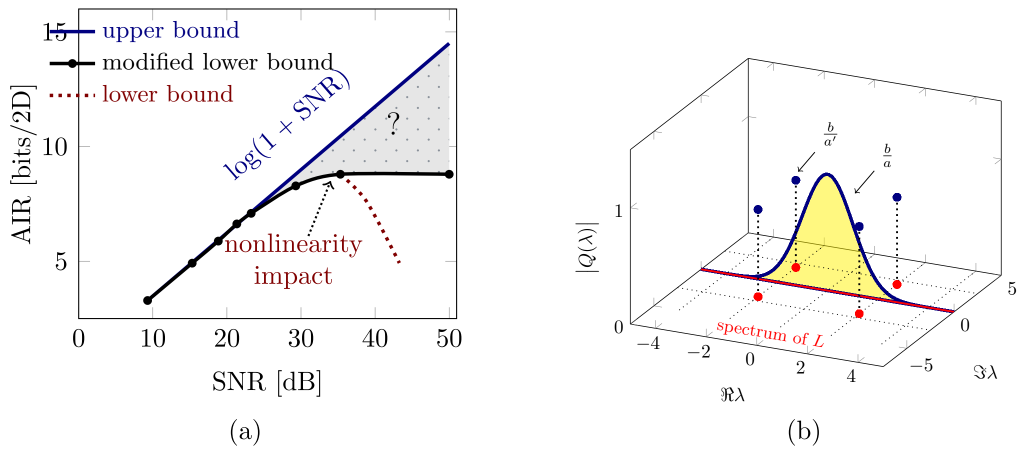

Fig. 2. (a) Capacity bounds; (b) the absolute value of the NFT as a function of complex frequency.

T is self-adjoint [3, Thm. 6]. In this basis, interactions in (4) are zero and

$$Y_\lambda = H_\lambda X_\lambda + N_\lambda, \tag{5}$$

where H_λ is an eigenvalue of T. As a result, the channel is decomposed into parallel independent scalar channels for $\lambda = 1, 2, \cdots$.

Interactions in (4) arise if the basis used for communication is not compatible with the channel. As a special case, let $\mathcal{H} = L_p^2([0, \mathcal{T}])$ and T be the convolution map $T(X) \triangleq H(t) * X(t)$, where $H(t) \in L^1(\mathbb{R})$ is the channel filter and $*$ denotes convolution. The eigenvectors and eigenvalues of T are

$$\phi_\lambda(t) = \frac{1}{\sqrt{\mathcal{T}}} \exp(-j\lambda\omega_0 t), \quad \omega_0 \triangleq \frac{2\pi}{\mathcal{T}},$$

and $H_\lambda \triangleq \mathcal{F}(H)(\lambda\omega_0)$. The Fourier transform maps convolution to a multiplication operator according to (5), where X_λ, Y_λ and N_λ are Fourier series coefficients. Interference and ISI are absent in the Fourier basis. OFDM is a technology in which information is modulated in independent spectral amplitudes X_λ, $\lambda \in \mathbb{N}$.

We explain NFDM in analogy with OFDM. First, we define the NFT as follows. Consider the operator

$$L \triangleq j \begin{pmatrix} \frac{\partial}{\partial t} & -q(t) \\ sq^*(t) & -\frac{\partial}{\partial t} \end{pmatrix}, \tag{6}$$

where $q(t) \in L^1(\mathbb{R})$ is the signal. Let $\mathbf{v}(\lambda, t) \triangleq [v_1, v_2]^T$ be an eigenvector of L corresponding to the eigenvalue λ, *i.e.*,

$$L\mathbf{v} = \lambda \mathbf{v}. \tag{7}$$

The eigenvalues λ of L are called *nonlinear frequencies*. They are complex numbers whose real and imaginary parts have physical significance [1, Ex. 1]. Define the normalized eigenvector

$$\mathbf{u}(t, \lambda) \triangleq \begin{pmatrix} a(t, \lambda) \\ b(t, \lambda) \end{pmatrix},$$

where

$$a \triangleq e^{j\lambda t}v_1, \quad b \triangleq e^{-j\lambda t}v_2, \tag{8}$$

with the initial condition $\mathbf{u}(-\infty, \lambda) = \begin{pmatrix}1, 0\end{pmatrix}^T$. The nonlinear Fourier coefficients are $a(\lambda) \triangleq a(\infty, \lambda)$ and $b(\lambda) \triangleq b(\infty, \lambda)$. The value of the NFT at the nonlinear frequency $\lambda \in \mathbb{R}$, called the *spectral amplitude*, is $b(\lambda)/a(\lambda)$.

If λ is a simple eigenvalue in the upper half complex plane $\mathbb{C}^+$, it can be shown that $a(\lambda) = 0$. As a result, the spectral amplitude for $\lambda \in \mathbb{C}^+$ is b/a', where prime denotes differentiation. It can be shown that $a(\lambda)$ is an analytic function of λ in $\mathbb{C}^+$ [3, Lem. 4]. Thus, nonlinear frequencies in $\mathbb{C}^+$ consist of the discrete set of (simple) zeros of $a(\lambda)$ denoted by $(\lambda_i)_{i\in\mathcal{N}}$, where $\mathcal{N} \triangleq \{1, \cdots, N\}$, $N \in \mathbb{N}$. If $s = 1$, the operator L is self-adjoint; thus $\mathcal{N}$ is empty and nonlinear frequencies are real.

To summarize, the NFT of $q(t) \in L^1(\mathbb{R})$ with respect to the L operator (6) is a function $Q(\lambda)$ of the complex frequency $\lambda \in \mathbb{C}$, defined as

$$Q(\lambda) \triangleq \begin{cases} \dfrac{b(\lambda)}{a(\lambda)}, & \lambda \in \mathbb{R}, \\ \dfrac{b(\lambda_i)}{a'(\lambda_i)}, & \lambda_i \in \mathbb{C}^+, \quad i \in \mathcal{N}. \end{cases}$$

The functions $\hat{q}(\lambda) \triangleq Q(\lambda)$, $\lambda \in \mathbb{R}$, and $\tilde{q}(\lambda_i) \triangleq Q(\lambda_i)$, $\lambda_i \in \mathbb{C}^+$, are called, respectively, the continuous and discrete spectrum.

Let $Q(\lambda, z)$ be the NFT of $q(t, z)$ with respect to t. The important property of the NFT is that, if $q(t, z)$ propagates in (1) with noise set to zero, we have

$$Q(\lambda, \mathcal{L}) = H(\lambda, \mathcal{L})Q(\lambda, 0), \tag{9}$$

where $H(\lambda, \mathcal{L}) \triangleq \exp(j4s\lambda^2\mathcal{L})$ is the all-pass-like channel filter. It follows that, just as the Fourier transform converts a linear convolutional channel into a number of parallel independent channels in frequency, the NFT converts the nonlinear dispersive channel (1) in the absence of noise into a number of parallel independent channels in nonlinear frequency. In NFDM information is modulated in independent spectral amplitudes $\mathrm{Q}(\lambda)$ for every λ.

4.2 Review of the NFDM

We consider a multi-user system with N_u users and N_s symbols per user. Linear and nonlinear (passband) bandwidths are denoted, respectively, by B and W. Users operate in equally-spaced non-overlapping intervals of width $W_0 \triangleq W/N_u$ Hz in the nonlinear frequency $l \triangleq \lambda/2\pi$. User k is centered at the nonlinear frequency $l = kW_0$ and operates in the nonlinear frequency interval

$$\mathcal{W}_k \triangleq \big[kW_0 - \frac{W_0}{2}\,,\, kW_0 + \frac{W_0}{2}\big], \quad k_1 \leqslant k \leqslant k_2.$$

where $k_1 \triangleq -\left\lfloor \frac{N_u}{2} \right\rfloor$ and $k_2 \triangleq \left\lceil \frac{N_u}{2} \right\rceil - 1$, in which $\lfloor x \rfloor$ and $\lceil x \rceil$ denote, respectively, rounding $x \in \mathbb{R}$ to nearest integers towards minus and plus infinity.

4.2.1 NFDM Transmitter

Let $(\Phi_\ell(\lambda))_{\ell=\ell_1}^{\ell_2}$ be an orthogonal basis for signals supported on $\mathcal{W}_0$ in the nonlinear frequency domain. NFDM begins with computing the signal

$$U(\lambda, 0) \triangleq \underbrace{\sum_{k=k_1}^{k_2}}_{\text{linear mux}} \underbrace{\left(\sum_{\ell=\ell_1}^{\ell_2} s_\ell^k \Phi_\ell(\lambda - 2\pi k W_0) \right)}_{\text{linear mod.}}, \tag{10}$$

where $(s_\ell^k)_{\ell=\ell_1}^{\ell_2}$ are symbols of the user k drawn from a constellation Ξ.

Taking the inverse Fourier transform $\mathcal{F}^{-1}$ of (10) with respect to λ

$$u(\tau, 0) \triangleq \sum_{k=k_1}^{k_2} \left(\sum_{\ell=\ell_1}^{\ell_2} s_\ell^k \phi_\ell(\tau) \right) e^{j2\pi k W_0 \tau}, \tag{11}$$

where $\phi_\ell(\tau) \triangleq \mathcal{F}^{-1}\big(\Phi_\ell(\lambda)\big)$, $\|\phi_\ell(\tau)\| = 1$. The variable τ can be interpreted as the *nonlinear time* (measured in seconds), the Fourier-conjugate of the nonlinear frequency $l = \lambda/2\pi$ (measured in Hz). Typically,

$$\phi_\ell(\tau) \triangleq \phi(\tau - \ell T_0), \tag{12}$$

where the pulse shape $\phi(\tau)$ and T_0 are chosen so that $|\mathcal{F}(\phi)(f)|^2$ satisfies the Nyquist zero-ISI criterion for T_0.

Given $U(\lambda, 0)$, the transmitted NFT signal is

$$\hat{q}(\lambda, 0) = \left(s - s e^{-\frac{s}{2}|U(\lambda,0)|^2} \right)^{\frac{1}{2}} e^{j\mathrm{Arg}(U(\lambda,0))}, \tag{13}$$

where $U(\lambda, 0) = \mathcal{F}(u(\tau, 0))$. The transformation (13) ensures that the signal energy in time, frequency, nonlinear time and nonlinear frequency are the same, which is convenient for modulation. Finally, the signal is computed in the time domain using the inverse NFT (INFT)

$$q(t, 0) = \mathrm{INFT}(\hat{q}(\lambda, 0)),$$

and sent over the channel.

4.2.2 NFDM Receiver

At the receiver, first the NFT is applied to $q(t, \mathcal{L})$ to obtain $\hat{q}(\lambda, \mathcal{L})$. Then, channel equalization is performed

$$\hat{q}_e(\lambda, \mathcal{L}) \triangleq H^{-1}(\lambda, \mathcal{L}) \hat{q}(\lambda, \mathcal{L}), \tag{14}$$

where $H(\lambda, \mathcal{L})$ is the channel filter in (9). Next, $U_e(\lambda, \mathcal{L})$ is computed from $\hat{q}_e(\lambda, \mathcal{L})$ according to the inverse of the transformation (13)

$$U_e(\lambda, \mathcal{L}) \triangleq \left(-2s \log(1 - s\,|\hat{q}(\lambda, \mathcal{L})|^2) \right)^{\frac{1}{2}} e^{j\mathrm{Arg}(\hat{q}(\lambda, \mathcal{L}))}, \tag{15}$$

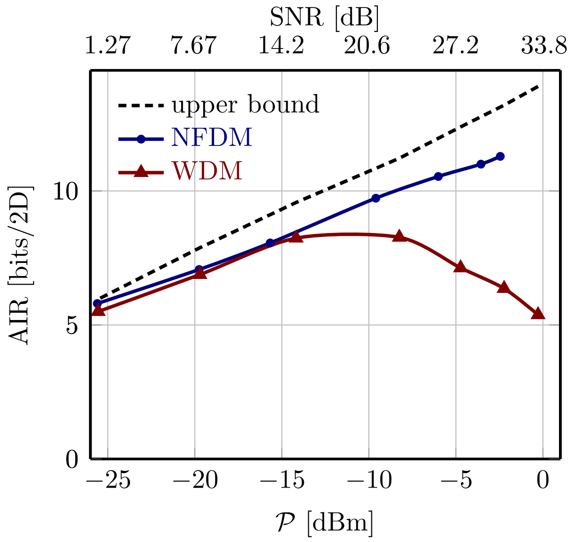

Fig. 3. The AIRs of NFDM and WDM, and the capacity upper bound.

where $\mathrm{Arg}(\hat{q})$ is the phase of $\hat{q}$. Finally, the received symbols are

$$\hat{s}_\ell^k = \frac{1}{2\pi} \int_{-\infty}^{\infty} U_e(\lambda, \mathcal{L}) \Phi_\ell^*(\lambda - 2\pi k W_0) \mathrm{d}\lambda. \tag{16}$$

Alternatively, $u_e(\tau, \mathcal{L}) \triangleq \mathcal{F}^{-1}(U_e(\lambda, \mathcal{L}))$ can be computed. The received symbols at the output are obtained by match filtering

$$\hat{s}_\ell^k = \int_{-\infty}^{\infty} u_e(\tau, \mathcal{L}) \phi_\ell^*(\tau) e^{-j2\pi k W_0 \tau} \mathrm{d}\tau.$$

5 Comparison of the Achievable Rates

In this section, we compare the AIRs of WDM and NFDM in the defocusing regime, subject to the same bandwidth and average power constraints.

We consider an optical fiber network with the standard single-mode fiber, with the loss coefficient $\alpha = 0.046$ km^{-1}, chromatic dispersion $D = 17$ ps/(nm−km) and nonlinearity parameter $\gamma = 1.27$ (W.km)$^{-1}$. The power spectral density of the amplified spontaneous emission (ASE) noise arising from the distributed Raman amplification is $\sigma_0^2 \triangleq 6.48 \times 10^{-21}$ W/(km.Hz).

We consider a simple network consisting of a link with 2000 km, one ADM at TX and one at RX. The ADM at RX is a filter in the frequency in WDM, and a filter in the nonlinear frequency in NFDM. In WDM, back-propagation is applied to the filtered signal according to the NLS equation. The corresponding equalization in NFDM is given by (14). To keep the computational complexity manageable, we choose $N_u = 5$ and $N_s = 1$. The results have been extended by FONTE researchers to larger values of N_u and N_s. The total linear bandwidth is $B = 100$ GHz, and the pulse shape $\phi(\tau)$ is root raised cosine with 25 % excess bandwidth.

We approximate the channel after equalization by the discrete memoryless channel $s_0^0 \mapsto \hat{s}_0^0$ in the linear or

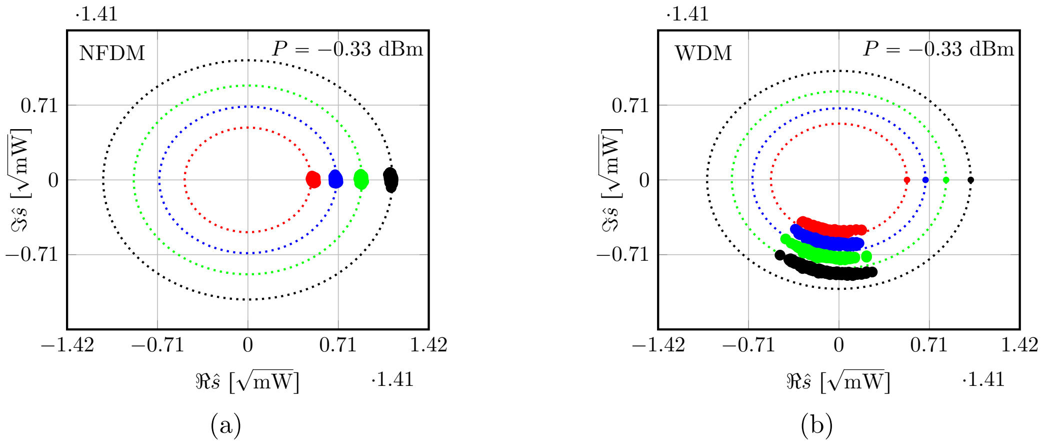

Fig. 4. Received symbols for four transmitted symbols in (a) NFDM, and (b) WDM.

nonlinear frequency. The AIR at the average signal power $\mathcal{P}$ is defined as the maximum of the mutual information over the probability distribution $p(s_0) \triangleq p_{S_0}(s_0)$:

$$\begin{aligned} R(\mathcal{P}) &\triangleq \max_{p(s_0)} \ I(s_0; \hat{s}_0), \\ \mathsf{E}|s_0|^2 &= \mathcal{P}, \end{aligned}$$

measured in bits per two real (one complex) dimensions (bits/2D) [8, Chap. 2]. The constellation Ξ consists of $N_r = 32$ or 64 rings each with $N_\phi = 128$ phase points. The number of signal samples in time and nonlinear frequency is $N = M = 16384$. We estimate the transition probabilities $s_0^0 \mapsto \hat{s}_0^0$ based on 4000 simulations of the stochastic NLS equation.

Fig. 3 shows the AIRs of NFDM and WDM. As expected, the WDM AIR characteristically vanishes as the input power is increased more than an optimal value $\mathcal{P}^* \approx -10$ dBm. In contrast, the NFDM AIR continues to increase for $\mathcal{P} > \mathcal{P}^*$ — at least up to the maximum power in Fig. 3 where we could perform simulations. The channel capacity is upper bounded by $\log_2(1 + \text{SNR})$, where $\text{SNR} = \mathcal{P}/(\sigma_0^2 B\mathcal{L})$ is the signal-to-noise ratio. This upper bound in Fig. 3 is not a perfect straight line, because the power in the horizontal axis is based on the 99% time duration.

Fig. 4 (a) shows the received symbols corresponding to four transmitted symbols in NFDM. The size of the 'clouds" does not increase notably as $|s_0^0|$ is increased. The corresponding constellation in WDM at the same power is presented in Fig. 4(b). The WDM clouds in Fig. 4(b) are bigger than the NFDM clouds in Fig. 4(a). Note that in WDM, there is a rotation of symbols, even after back-propagation. This rotation, which is about $\gamma\mathcal{L}\mathcal{P}$ (γ being the nonlinearity coefficient), is due to the cross-phase modulation; see [9, Eq. 21].

6 Conclusions

We briefly reviewed the linear and nonlinear frequency division multiplexing in fiber-optic communication. It was shown that the NFDM AIR is greater than the WDM AIR for a given power and bandwidth, in an integrable model of the optical fiber in the defocusing regime, and in a representative system with one symbol per user. While the work serves as a good starting point, further research on the nonlinear multiplexing is needed.

References

[1] M. I. Yousefi and F. R. Kschischang, "Information transmission using the nonlinear Fourier transform, Part III: Spectrum modulation," *IEEE Trans. Inf. Theory*, vol. 60, no. 7, pp. 4346–4369, Jul. 2014.

[2] M. I. Yousefi and X. Yangzhang, "Linear and nonlinear frequency-division multiplexing," arXiv:1603.04389, pp. 1–14, Mar. 2016. [Online]. Available: http://arxiv.org/abs/1603.04389

[3] M. I. Yousefi and F. R. Kschischang, "Information transmission using the nonlinear Fourier transform, Part I: Mathematical tools," *IEEE Trans. Inf. Theory*, vol. 60, no. 7, pp. 4312–4328, Jul. 2014.

[4] ——, "Information transmission using the nonlinear Fourier transform, Part II: Numerical methods," *IEEE Trans. Inf. Theory*, vol. 60, no. 7, pp. 4329–4345, Jul. 2014.

[5] A. Splett, C. Kurtzke, and K. Petermann, "Ultimate transmission capacity of amplified optical fiber communication systems taking into account fiber nonlinearities," in *European Conf. Opt. Commun.*, Montreux, Switzerland, Sep 1993, pp. 41–44.

[6] R. J. Essiambre, G. Kramer, P. J. Winzer, G. J. Foschini, and B. Goebel, "Capacity limits of optical fiber networks," *IEEE J. Lightw. Technol.*, vol. 28, no. 4, pp. 662–701, Feb. 2010.

[7] E. Agrell, "Conditions for a monotonic channel capacity," *IEEE Trans. Commun.*, vol. 63, no. 3, pp. 1–11, Sep. 2015.

[8] G. D. Forney, Jr., "Principles of digital communication II." Massachusetts Institute of Technology, Mar. 2005, MIT OpenCourseWare, Course no. 6.451, Lecture Notes.

[9] M. I. Yousefi, "The Kolmogorov-Zakharov model for optical fiber communication," *IEEE Trans. Inf. Theory*, vol. 61, no. 1, pp. 377–391, Jan. 2017.